DOI: 10.1002/chem.200601205

Water-Soluble Self-Assembled Butadiyne-Bridged Bisporphyrin: A Potential Two-Photon-Absorbing Photosensitizer for Photodynamic Therapy

Joanne T. Dy, Kazuya Ogawa, Akiharu Satake, Atsushi Ishizumi, and Yoshiaki Kobuke*[a]

Abstract: We have synthesized a novel, two-photon-absorbing photosensitizer for two-photon-absorption photodynamic therapy (2PA-PDT). The molecule is a butadiyne-bridged porphyrin dimer terminated with two water-soluble porphyrin monomers connected through Zn-imidazolyl self-assembly and covalently linked through olefin metathesis. It has an effective two-photon-absorption (2PA) cross-section value, $\sigma^{(2)}$, of $33\,000 \pm 4600$ GM with 5-ns pulses at 890 nm measured by using the open-aperture *Z*-scan technique. The compound was found to generate singlet oxygen, cytotoxic for tumor cells in photodynamic therapy (PDT), under 2PA conditions by conducting photobleaching experiments with anthracene-9,10-dipropionic acid sodium salt (ADPA).

Keywords: photodynamic therapy · porphyrins · self-assembly · singlet oxygen · two-photon absorption

Introduction

Recent interdisciplinary attention has focused on nonlinear optical materials, especially those with efficient two-photon absorption due to their numerous potential applications such as two-photon photodynamic therapy,[1] optical power limiting,[2] ultrahigh-density optical-data storage,[3] two-photon-excited fluorescence spectroscopy,[4] and three-dimensional (3D) microfabrication.[5]

Two-photon absorption (2PA) is a third-order nonlinear phenomenon in which excitation occurs by the simultaneous absorption of two photons at comparatively long wavelengths instead of by a single-photon excitation at a shorter wavelength.[6] Typically, a chromophore reaches its excited state (S_n) through excitation at its one-photon wavelength λ. However, S_n excitation is also possible at wavelength 2λ by using strong laser pulses, whereby two photons are simultaneously absorbed by the molecule. The 2PA efficiency is quantified by the two-photon-absorption cross section $\sigma^{(2)}$ in GM, which corresponds to 10^{-50} cm^4 sec molecule^{-1} photon^{-1}. In 2PA, the photon absorbed contains only half of the nominal excitation energy and, therefore, penetrates absorbing or scattering media more effectively. The absorption at longer wavelengths, especially in the near-infrared (NIR) region, is vital for biological applications because it increases the penetration of tissues by light.[7] In addition, the quadratic dependence on the laser intensity permits spatial selectivity by using a focused laser beam.[8]

A wide variety of 2PA materials have been developed by using both organic and inorganic materials. The most efficient of these materials are composed of donor and acceptor molecules linked by a conjugated π bridge.[9] Some of the π bridges that have been studied so far are *trans*-stilbene,[9a] fluorene,[9b] dithienothiophene,[9c] and butadiyne[9d,e] linkers. Increasing the length of the molecules also results in a substantial increase in $\sigma^{(2)}$. Porphyrins that have highly conjugated π systems are also attractive candidates for 2PA materials. Another important feature of porphyrins is the easy functionalization of their *meso* and β positions. Hydrophobic or hydrophilic moieties can be affixed to alter the solubility of the porphyrin ring without altering its vital properties. However, monomeric porphyrins exhibit small cross-section values of less than tens of GM.[10]

We have previously reported a butadiyne-linked bisporphyrin dimer with a strong $\sigma^{(2)}$ value of 7600 GM with femtosecond pulses at 870 nm.[11] Two porphyrins were connected by a butadiyne bridge that assumes a cumulenic structure upon photoexcitation, allowing a highly conjugated planar

[a] J. T. Dy, Prof. K. Ogawa, Prof. A. Satake, Prof. A. Ishizumi, Prof. Y. Kobuke
Graduate School of Materials Science
Nara Institute of Science and Technology
8916-5 Takayama, Ikoma, Nara 630-0101 (Japan)
Fax: (+81) 743-72-6119
E-mail: kobuke@ms.naist.jp

Supporting information for this article is available on the WWW under http://www.chemeurj.org/ or from the author and includes calculations and detailed experimental diagrams and data.

structure. We also discovered that the slipped cofacial arrangement by complementary coordination of imidazolyl to zinc[12] can effectively increase $\sigma^{(2)}$ almost four fold. Anderson and co-workers have also investigated several acetylene-bridged zinc-inserted porphyrin dimers with promising two-photon-absorption cross sections in the near-infrared regions, reaching values of 1×10^4 GM in the region of 820–890 nm.[13]

The field of photodynamic therapy (PDT) can benefit enormously from 2PA. PDT is a light-activated treatment used to destroy tumor cells, particularly in the skin, throat, and lungs.[14] In PDT, a drug called a photosensitizer (PS) is injected into the body and localizes to the tumor. On its own, a photosensitizer is not active; however, upon irradiation with laser light, it generates triplet states (^{3}PS*) through intersystem crossing. This, in turn, reacts with ground-state molecular oxygen ($^3O_2$), which is in its triplet state, producing cytotoxic singlet-oxygen species responsible for the destruction of the tumor cells. One of the major problems of currently available PSs is their excitation wavelength of around only 630 nm, which reduces the cellular transmission of laser light.[15] In 2PA, excitation can be performed at longer wavelengths, which is beneficial for PDT because the absorption within the optical window of biological tissues in the range of 700–1500 nm is increased.[16] Moreover, the quadratic dependence on the laser intensity requires a focused laser beam for excitation, which in turn allows high spatial selectivity, keeping the healthy tissues safe and intact. This ideal combination is known as two-photon-absorption photodynamic therapy (2PA-PDT).

Ogilby and co-workers have recently reported singlet-oxygen generation from several monomeric porphyrin-,[17a] phenyl-vinylene-,[17b,c] and phenylene-ethynylene-based[17d] photosensitizers by two-photon excitation. Two-photon excitation at 780 nm has also been applied to cells treated with aminolevulinic acid and protoporphyrin for photosensitization.[18a] Oh and co-workers have demonstrated the generation of singlet oxygen by spatially controlled two-photon excitation in fibroblasts by using 5-chloromethyl-2′,7′-dichlorodihydrofluorescein diacetate acetyl ester.[18b]

We also reported potential 2PA-PDT agents with large effective 2PA cross sections, good yields for one-photon-excited singlet-oxygen yields, and PDT by using one-photon irradiation.[14f] These compounds were acetylene-bridged bisporphyrins bearing carboxylates at their 10- and 20-*meso* positions. Herein, we report a different approach to building a water-soluble, two-photon-absorbing porphyrin-based photosensitizer (**1**) as a potential candidate for 2PA-PDT. A butadiyne-bridged bisporphyrin, known for possessing large 2PA cross sections, was chosen as the heart of this 2PA-PDT system. Unlike the previous compounds, a dendritic residue was selected for hydrophilicity. Dissolving a large organic structure such as porphyrin requires a relatively large number of hydrophilic substituents. Thus, a porphyrin bearing six carboxylate units, as provided by the Newkome-type dendrimer,[19a] was attached at both ends of the butadiyne bisporphyrin through zinc-imidazolyl coordination to form a tetramer. To permanently link the coordinated structure, the allyl ether side chains were introduced to fix the structure through olefin metathesis.[19b] This overall procedure results in an average of three carboxylate units per porphyrin in the hope that this large porphyrin array is not only soluble in water, but also that the bulkiness of the terminal dendritic arms can increase hydrophilicity and eventually help the delivery of the photosensitizer to the tumor cells. In contrast to the previously reported compounds, the hydrophilic groups in compound **1** are larger in number and are located only at both ends of the tetramer. These factors may potentially affect drug delivery to the cells.

Results and Discussion

Design and synthesis: The molecule is composed of two parts that have different roles: the 2PA component, a zinc-

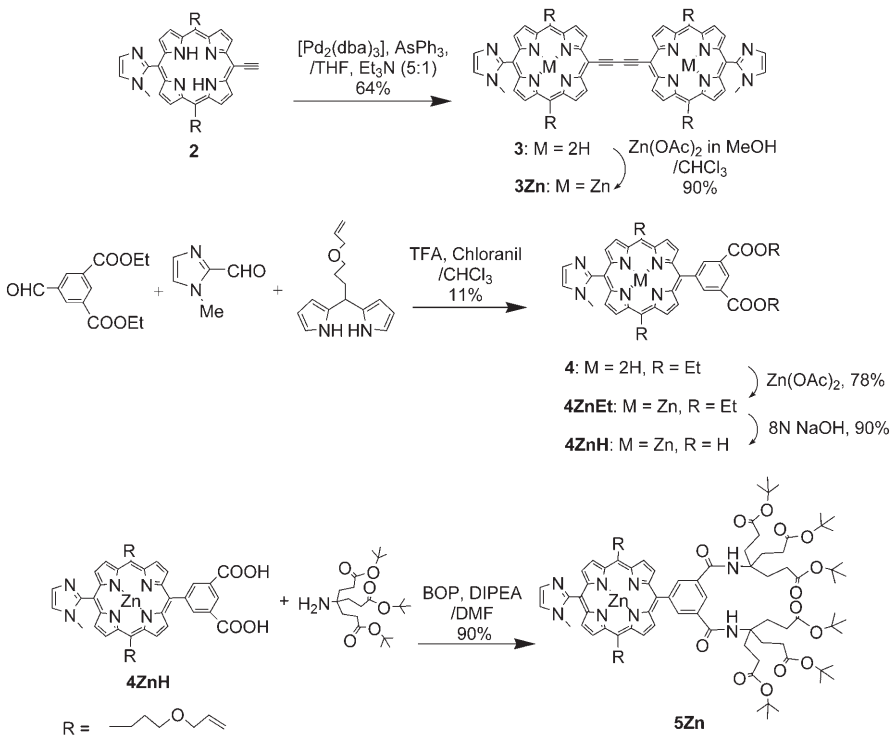

Scheme 1. Synthetic route to the 2PA (**3Zn**) and water-soluble (**5Zn**) components.

inserted butadiyne-bridged imidazolylporphyrin dimer **3Zn**, and the water-soluble component, a zinc-inserted isophthalamidoimidazolylporphyrin bearing 12 carboxylic acid groups, **5Zn**, The synthetic routes for these components are shown in Scheme 1.

The butadiyne-bridged porphyrin dimer was synthesized by palladium-catalyzed C–C bond formation of **2** by reaction with $[Pd_2(dba)_3]$ (dba = dibenzylideneacetone) and triphenylarsine to afford **3** in 64% yield. Freebase **3** was treated with zinc acetate to give the 2PA component, a zinc-inserted butadiyne-bridged porphyrin, **3Zn**, in 90% yield. To increase hydrophilicity, the water-soluble component **4ZnH** was appended with a Newkome-type dendrimer through BOP (benzotriazol-1-yloxytris(dimethylamino)phosphoniumhexafluorophosphate) condensation, giving a total of six ester groups for compound **5Zn** in 90% yield.

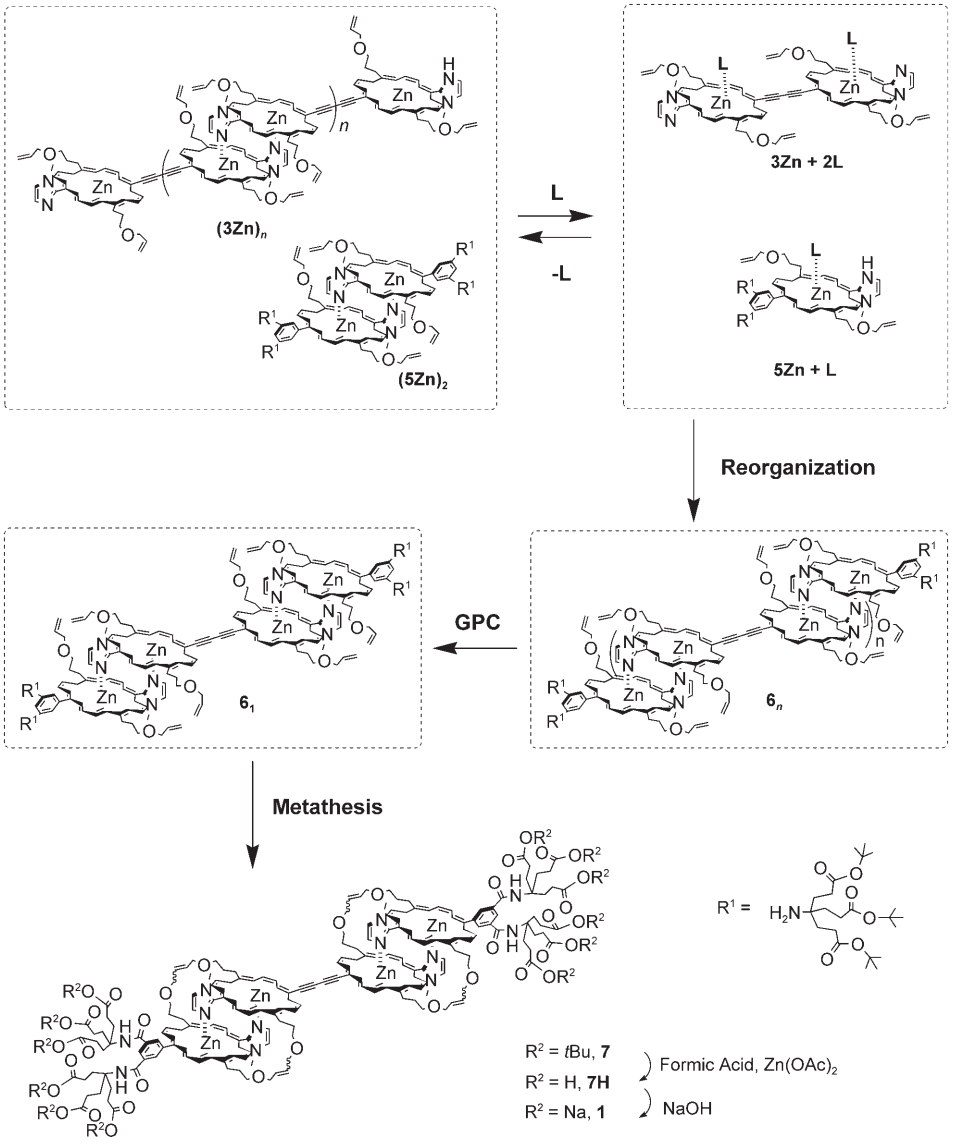

Scheme 2. Synthetic route to the water-soluble 2PA porphyrin tetramer **1**. (L = methanol or pyridine)

In noncoordinating solvents such as $CHCl_3$ and toluene, these porphyrins **3Zn** and **5Zn** exist as polymer $(\mathbf{3Zn})_n$ and as dimer $(\mathbf{5Zn})_2$, respectively, due to the complementary coordination of imidazolyl to the central zinc metal of the porphyrin, as shown in Scheme 2.[20] However, in coordinating solvents such as pyridine and methanol, porphyrins **3Zn** and **5Zn** are in their monomeric form. To form the desired tetramer $\mathbf{6_1}$, this coordination should initially be dissociated by dissolving a 2:1 molar mixture of **5Zn**/**3Zn** in pyridine. Reorganization took place as pyridine was gradually removed by evaporation, wherein different length arrays of $(\mathbf{3Zn})_n$ terminated with monomer **5Zn** at both ends were formed ($\mathbf{6}_n$). This oligomeric mixture, $\mathbf{6}_n$, exists in a statistical ratio, as observed from gel-permeation chromatography (GPC) (Figure 1, left).

Tetrameric compound $\mathbf{6_1}$ was separated by using preparative GPC. In this study, only the tetramer fraction was selected because of its better solubility in water after hydrolysis. Other fractions are interesting in view of the extended length of the π systems and will be characterized in the future. The collected fraction is relatively stable if dissolved in noncoordinating solvents. However, it may still undergo gradual reorganization, thus, it is imperative to permanently fix the structure through metathesis of the allyl ether side chains by using the Grubbs catalyst, to finally give the meta-

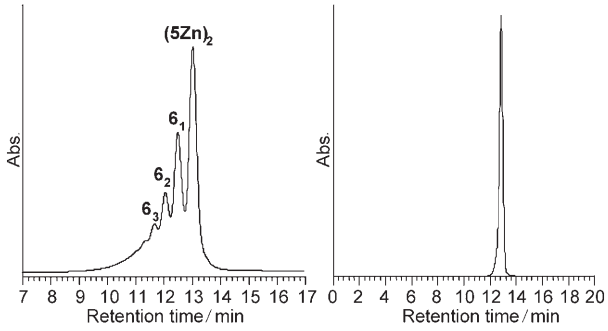

Figure 1. Analytical GPC charts of (left) $(\mathbf{5Zn})_2$ and $\mathbf{6}_n$ (n = 1,2,3, etc.), a reorganized 2:1 mixture of **5Zn**:**3Zn**; (right) **7**, retention time = 12.85 min (JAIGEL 3H-A; eluent: $CHCl_3$; flow rate: 1.2 mL min^{-1}).

thesized target compound **7**. The length of the side chain necessary for metathesis has been reported.[19b] The purity of tetramer **7** is evident from the strong isolated peaks of its analytical GPC (Figure 1, right) and MALDI-TOF mass profiles (Figure 2). In Figure 1, tetramer **7** shows a single

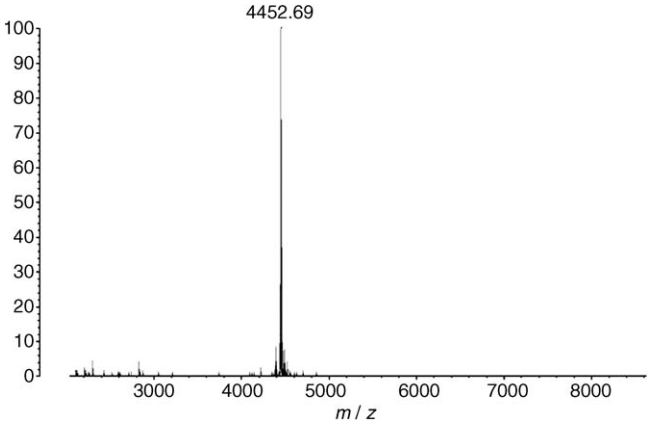

Figure 2. The MALDI-TOF mass spectrum of **7** shows the target peak at $m/z = 4452.69$.

peak with a retention time of 12.85 min excluded from other peaks. The effective mass value of compound **7**, $m/z =$ 4452.69, is also in good agreement with the calculated mass for $C_{244}H_{290}N_{28}O_{36}Zn_4$ of 4452.20. This is further evidenced in the ^{1}H NMR peaks that were assigned according to $\{^1H,^1H\}$ COSY two-dimensional (2D) NMR spectra (see Supplementary Information).

Because **7** possesses an average of three carboxylate groups per porphyrin unit, it may be sufficient to dissolve this large compound in water. The treatment of compound **7** with formic acid cleaves all twelve *t*Bu groups to form the carboxylic acid tetramer **7H** and can be followed by treatment with an equimolar amount of NaOH to finally yield the water-soluble tetramer **1**.

Photophysical characterization: **5Zn**, **5Zn+Im**, and **3Zn+2Im** (Im = methylimidazole) exhibit the typical absorption spectra of a slipped-cofacial dimer,[12] a coordination-cleaved monomer,[12] and a butadiyne porphyrin,[21] respectively, as shown in Figure 3. However, the absorption spectrum of metathesized tetramer **7** (Figure 4) is not a simple superposition of the two individual components. Its unique absorption spectrum results from the excitonic coupling of the B_x, B_y, and B_z dipole moments of the terminal monomer and central dimer porphyrins. Peak $\mathbf{P_0}$ at 434 nm can be attributed to the freely rotating face-to-face interactions of all the B_y and B_z moments. It spans from the orthogonal conformation of the butadiyne-linked bisporphyrin ($B_{1y}B_{2y}$ and $B'_{1z}B'_{2z}$) to the parallel conformation ($B_{1y}B_{2y}B'_{2y}B'_{1y}$), resulting in the blue-shifted band. As mentioned previously, no interruption of the conjugation path occurs between the two porphyrin units of the butadiyne dimer through the butadiyne axis, and its two interacting B_x dipole moments can be considered as

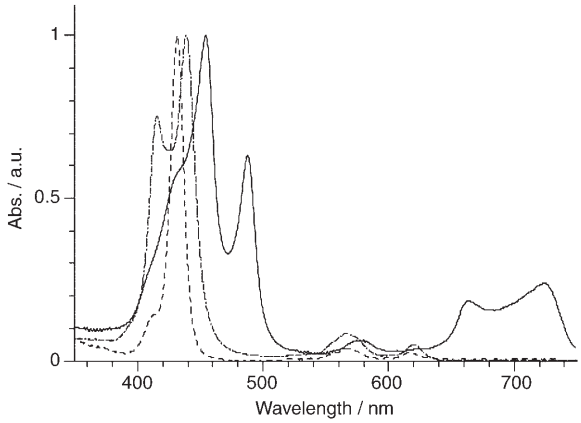

Figure 3. Absorption spectra of $(\mathbf{5Zn})_2$ (–•–•), **5Zn+Im** (– – –) and **3Zn+2Im** (——) in $CHCl_3$.

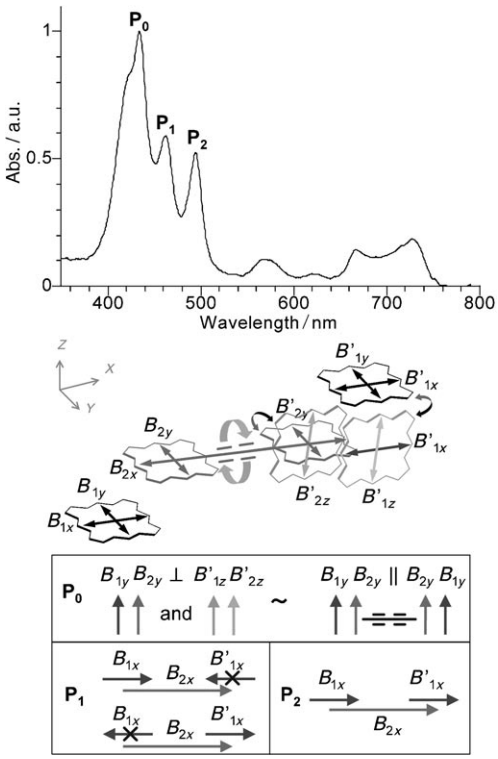

Figure 4. Absorption spectrum of **7** in $CHCl_3$ (top) and excitonic coupling of porphyrins in metathesized tetramer **7** (bottom).

a single "long" dipole moment (B_{2x}). The most red-shifted peak, $\mathbf{P_2}$, at 495 nm can be attributed to the head-to-tail interactions of all the B_x dipole moments (i.e., $B_{1x}B_{2x}B'_{1x}$). The orientations of the porphyrins are unimportant because all of the B_x moments are parallel to each other and all the center-to-center distances of the adjacent B_x moments are equal. Thus, the remaining peak $\mathbf{P_1}$ at 463 nm can be assigned to the $B_{1x}B_{2x}$ interaction.

The emission spectra of compounds **5Zn+Im**, **3Zn+2Im**, and **7** are shown in Figure 5. The emission intensities are normalized according to the absorbance of the com-

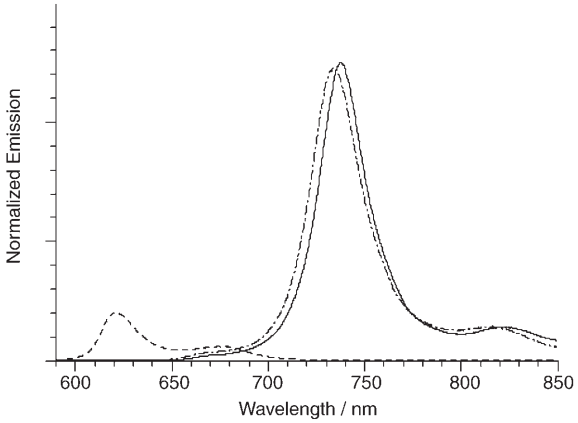

Figure 5. Fluorescence spectra of **5Zn+Im** (– – –), **3Zn+2Im** (–•–•–), and metathesized tetramer **7** (——) in $CHCl_3$.

pounds at their respective excitation wavelengths. At 566 nm excitation, porphyrin monomer **5Zn+Im** gave two emission peaks at 632 and 680 nm. On the other hand, stronger and extremely red-shifted peaks at 734 and 817 nm were observed for the butadiyne-bridged porphyrin dimer **3Zn+2Im** upon 577 nm irradiation. Interestingly, in the emission spectrum of **7**, the fluorescence component corresponding to the terminal part observed in dimer **5Zn+Im** was completely quenched and emitted from only the 2PA part, accompanied by a slight increase in the peak intensity relative to that of monomer **3Zn+2Im**. Taking into account the complete overlap of the emission bands of compound **5Zn+Im** with the absorption bands of compound **3Zn+2Im** at around 600–700 nm, these effects are all indicative of fluorescence-resonance-energy transfer from the terminal monomer to the central porphyrin butadiyne-bridged dimer.[22] This is further supported by the excitation spectrum for **7** (see Supporting Information), which has a shape very similar to its absorption spectrum.

Finally, the absorption and fluorescence spectral shape of **1** are different from those of **7** in the relative oscillator strengths and emission intensities (Figure 6). This may be caused by aggregation that frequently occurs with porphyrins in water.[23] This is now under further investigation.

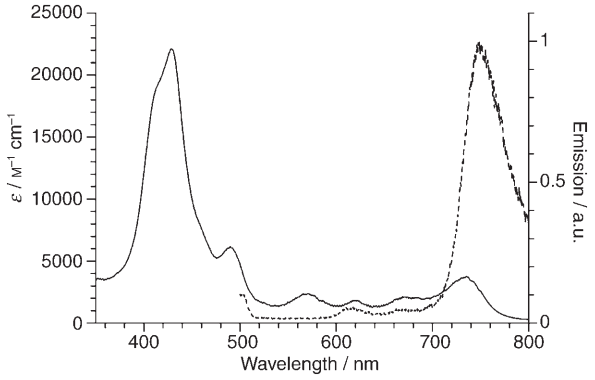

Figure 6. Absorption (——) and emission (– – –) spectra of **1** in water.

Two-photon absorption: The effective 2PA cross section was measured by using an open-aperture *Z*-scan technique with an Nd:YAG laser source. A 0.4-mM solution of compound **1** in water in a 1-mm cell was irradiated with 5-ns pulses at a repetition rate of 10 Hz.

A typical *Z*-scan trace of compound **1** in water at 890 nm with its theoretically fitted curve is shown in Figure 7, in

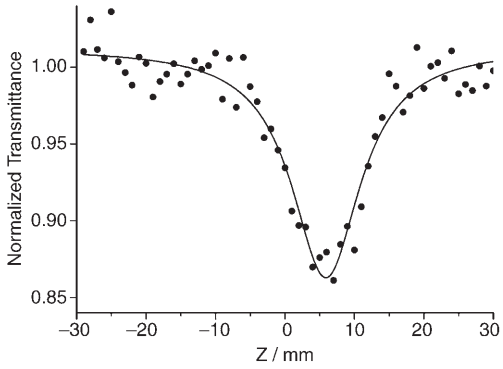

Figure 7. Typical *Z*-scan trace (●) and theoretically fitted curve (line) of 0.4 mM of **1**, pH 7.

which the normalized transmittance is plotted as a function of the sample position, *Z*. The curve fits were performed according to the theoretical expression for the transmittance.[9d,11] The effective 2PA spectrum of compound **1** in water is shown in Figure 8.

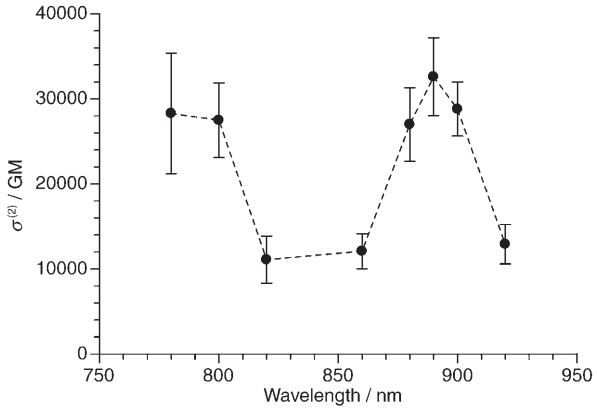

Figure 8. Two-photon absorption spectrum of 0.4 mM **1** in water, pH 7.

The real 2PA maximum peak for compound **1** appeared at 890 nm (11235 cm^{-1}), with a value of 33000 ± 4600 GM. It should be noted that it is difficult to compare this 2PA cross-section value with those obtained by different pulse widths. For instance, acetylene-bridged porphyrins have been reported to possess $\sigma^{(2)}$ values in the range of 10000 GM by using femtosecond pulses.[11,13b] The nanosecond values are approximately 30 times larger than the femtosecond values for our previously reported compounds.[11b] The large discrepancy between nanosecond and femtosec-

ond values is attributed to excited-state absorption (ESA) because of the longer pulse width in nanosecond lasers relative to those in femtosecond lasers. Furthermore, the ESA component is extremely difficult to separate from the pure 2PA signal.

However, the effective values obtained herein are clearly large compared to values of related compounds employing the same nanosecond pulses. The effective $\sigma^{(2)}$ value of compound **1** is almost three orders of magnitude larger than H_2TPP, 150-fold that of zinc-imidazolyl-coordinated porphyrin dimer, and twice that of an alkyl *meso*-substituted bisporphyrinatozinc(II) monomer, which have values of 29 GM (at 780 nm), 188 GM (at 780 nm), and 14000 GM (at 890 nm), respectively.[24] As reported previously, this increase in 2PA can be attributed not only to the increased number of porphyrins, but may also be due to the conjugated butadiyne π bridge that provides a pathway for strong electronic conjugation between the porphyrins. Additionally, the complementary coordination of porphyrins **3Zn** and **5Zn** also contributes to the increase in 2PA.[11] Moreover, the donor–acceptor configuration of compound **1** induces polarization within the molecule to enhance 2PA.[9]

Aggregation was probably present in the absorption spectrum because the Q bands were blue-shifted and the lower-energy Soret bands, which are mainly from the butadiyne bisporphyrin, showed an increase in oscillator strength upon the addition of pyridine (see Supporting Information). To determine the effect of aggregation on 2PA, the effective $\sigma^{(2)}$ value of compound **1** in water in the presence of excess pyridine at 890 nm was measured under the same experimental conditions. Compound **1** with pyridine gave a value of 36000 ± 5000 GM, which is almost equivalent to the value measured in water only. In addition, 2PA of compound **1** in water at different concentrations was measured. Figure 9

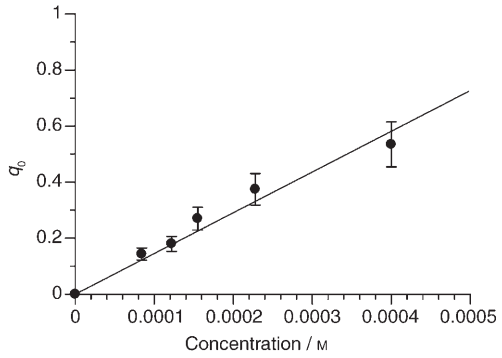

Figure 9. Linear dependence of the two-photon absorbance q_0 on the concentration of compound **1** in water, pH 7.

shows a plot of the two-photon absorbance q_0 with respect to concentration and clearly displays a linear relationship. From Equations (3) and (5) of the $\sigma^{(2)}$ calculations (see Supporting Information), the two-photon absorbance q_0 should be linearly proportional to the number density N, and consequently to the concentration. Thus, although aggregation is present in solution, $\sigma^{(2)}$ is not aggregation-dependent for compound **1**.

Singlet-oxygen generation by two-photon excitation: In PDT, cytotoxicity of the tumor cells is caused by singlet oxygen that is usually generated by energy transfer from the triplet state of the photosensitizer to ground-state oxygen. The amount of singlet oxygen generated can be determined quantitatively by using scavengers such as anthracene-9,10-dipropionic acid sodium salt (ADPA), which reacts with oxygen to form an endoperoxide. Therefore, a D_2O solution of ADPA and compound **1** was irradiated with 100-fs pulses at 890 nm with a peak power of 6.1 GW cm^{-2}. Although ADPA absorbs in the same region as the sensitizers, it exhibits characteristic vibrational peaks at 399, 378, 359, and 342 nm. Continuous photobleaching of anthracene absorption was observed for 3 h by using 890 nm excitation (Figure 10). In contrast, almost no change was observed in

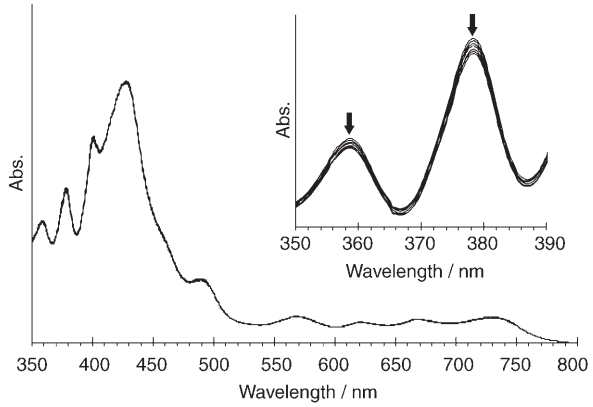

Figure 10. Photobleaching experiments of **1** after two-photon excitation at 890 nm in D_2O at RT. Inset: Magnification of continuous quenching of ADPA absorbance during the course of a 3-h exposure.

the Q bands of compound **1**, indicating that the sensitizer itself is not affected during either two-photon excitation or singlet-oxygen generation.

Almost no decrease in the anthracene absorbance was observed in the solutions without the sensitizer. The same experiment was undertaken by using tetrasulfonatophenylporphyrin (TPPS), which has very weak 2PA within these wavelength regions. The extent of quenching of the ADPA absorption peak at 379 nm by TPPS upon using compound **1** and TPPS is plotted in Figure 11a. It is clearly demonstrated that compound **1** is an effective photosensitizing agent under two-photon-excitation conditions. On the other hand, TPPS totally lacks this activity. To confirm that the decay of ADPA is due to the entrapment of singlet oxygen and not to other mechanisms, similar experiments were also performed in H_2O (Figure 11b). It is known that singlet oxygen in D_2O has a longer lifetime (60 μs) than in H_2O.[26,27] The difference in ADPA quenching between D_2O and H_2O is compatible with the expectation (Figures 11a and b, respectively).

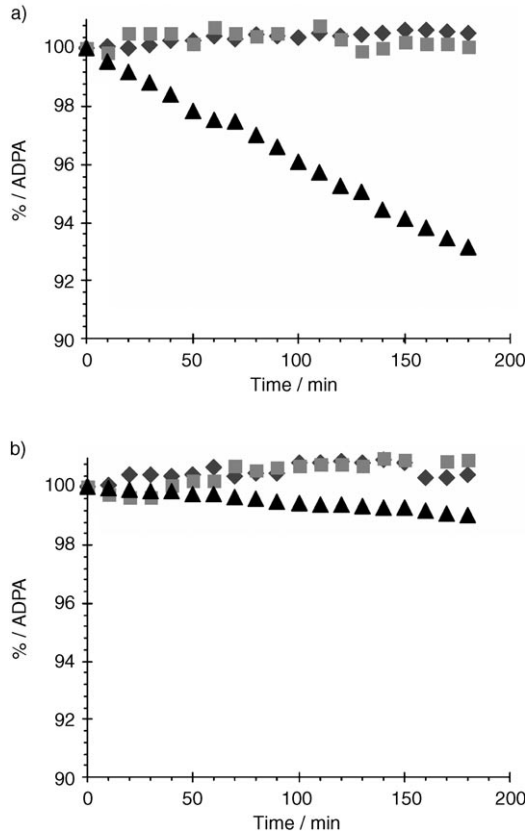

Figure 11. Photobleaching of the ADPA peak at 379 nm after two-photon-excited singlet-oxygen photosensitization at 890 nm: No photosensitizer (◆), TPPS (■), and **1** (▲) in a) D_2O and; b) H_2O.

Conclusion

A water-soluble two-photon-absorbing porphyrin tetramer **1** was successfully synthesized for the purpose of 2PA-PDT. A maximum effective 2PA cross-section value of 33000± 4600 GM was observed at 890 nm (full-width at half-maximum (FWHM) = 5 ns). This large effective $\sigma^{(2)}$ value relative to reference porphyrins measured under similar conditions can be attributed mainly to the butadiyne linker, which allows π conjugation between connected porphyrins. The increased two-photon absorption at the NIR wavelength is very beneficial for PDT applications, because the human body is relatively transparent to wavelengths within this region. Singlet oxygen was also successfully generated upon laser irradiation of this low-energy wavelength, as evidenced by ADPA photobleaching after two-photon excitation. Effective singlet-oxygen production upon two-photon irradiation qualifies compound **1** as an attractive photosensitizer candidate for two-photon photodynamic therapy, which will allow deeper-site tumor treatments due to its strong 2PA absorption at a longer wavelength of 890 nm. Cell studies for PDT are being actively pursued. Finally, it would be interesting to conduct a comparative study between compound **1** and the previously reported acetylene-bridged porphyrins[14f] to determine which type of structure and level of hydrophilicity will allow greater drug delivery into the tumor cells.

Experimental Section

General methods: ^{1}H and ^{13}C NMR spectra were obtained in $CDCl_3$, unless otherwise noted, with Me_4Si as the internal standard and were recorded by using either a JEOL JNM EX270 or JEOL ECP 600 spectrometer. IR spectra were obtained by using a Nicolet Avatar 320ES FTIR spectrometer. UV/Vis spectra were obtained by using either a Shimadzu UV-1650PC or UV-3100PC UV/Vis spectrophotometer. Fluorescence measurements were performed by using a Hitachi F-4500 fluorescence spectrophotometer. MALDI-TOF mass spectra were obtained by using a Perseptive Biosystems Voyager DE-STR and a Shimadzu/KRATOS Axima-CFR Kompact MALDI with dithranol and α-cyano-4-hydroxy cinnamic acid (Aldrich) as the matrix. Analytical GPC measurements were performed by using an HP Series 1100 with a JAIGEL 3H-A column. Reactions were monitored on silica gel 60 F_{254} TLC plates (Merck). The silica gel used for column chromatography was purchased from Kanto Chemical Co.: Silica Gel 60N (spherical, neutral) 60–210 and 40–50 μm (Flash). The alumina used for column chromatography was purchased from Merck: aluminum oxide 90 active basic.

All solvents and reagents were purchased and used without purification, unless indicated otherwise. Dry tetrahydrofuran (THF) was obtained by refluxing with sodium followed by distillation at 66 °C, atmospheric pressure, and stored over dry 4A molecular sieve (Nacalai). Dry dimethylformamide (DMF) was obtained by stirring with calcium hydride overnight and distilling in vacuo at 35 °C. Ethanol-free $CHCl_3$ was obtained by passing it through a short alumina column and was used only after storage for a short time over 4A molecular sieve (Nacalai).

Synthesis: 1-methyl-1*H*-imidazole-2-carbaldehyde,[28a] *meso*-(3-allyloxypropyl)dipyrromethane,[28b] 5,15-bis(3-allyloxypropyl)-10-ethynyl-20-(1′-methyl-2′-imidazolyl)porphyrin **2**,[28c] 5-hydroxymethylisophthalic acid diethyl ester,[28d] and tris(*tert*-butoxycarbonylpropyl)amine[19a] were synthesized according to published procedures. Pyridinium chlorochromate (PCC) was synthesized by reacting chromium trioxide (10 g, 0.1 mol) with a vigorously stirred HCl solution (6 N: 18.4 mL of 36% HCl in 11 mL H_2O, 0.11 mol) in a 100-mL beaker. After 5 min, the mixture was cooled to 0 °C and pyridine (8.1 mL, 0.1 mol) was added over 15 min through a dropping funnel. Upon addition of pyridine, the brown-violet solution coagulated into bright yellow-orange crystals. Pyridine was removed by vacuum filtration and dabbing with filter paper several times. It is important to remove all of the pyridine, otherwise, the obtained product will discolor and the reactivity will be reduced (15 g, 70%).

1,3-Bis(5-(15-(1-methyl-2-imidazolyl)-10,20-bis(3-allyloxypropyl)porphyrinyl))butadiyne (3): In a 100-mL flask, **2** (99 mg, 162 μmol) was dissolved in 5:1 v/v dry THF/TEA (11.4 mL). The solution was degassed with nitrogen by means of freeze–thaw cycles. Tris(dibenzylideneacetone) (chloroform)-di-palladium(0) ($[Pd_2(dba)_3]$, 1.36 mg, 8.1 μmol) and triphenylarsine ($AsPh_3$, 3.22 mg, 64.8 μmol) were added to the mixture under N_2 atmosphere. After stirring overnight at 35 °C, water was added and the mixture was extracted with $CHCl_3$. The organic layer was washed with brine, dried over anhydrous Na_2SO_4, and evaporated under reduced pressure. The resulting crude product was subjected to silica-gel chromatography for purification to elute compound **3** by using $CHCl_3$/MeOH (10:1 to 5:1 v/v); and $CHCl_3$/acetone (20% v/v) to $CHCl_3$/MeOH (10:1 v/v). Finally, the product was reprecipitated from $CHCl_3$ solution by the addition of *n*-hexane. The final product was vivid green in color (63.5 mg, 64%). R_f = 0.5 ($CHCl_3$/MeOH 10:1); ^{1}H NMR (270 MHz, $CDCl_3$): δ = 10.01 (d, J = 4.9 Hz, 2H; Por β), 9.63 (d, J = 4.9 Hz, 2H; Por β), 9.47 (d, J = 4.9 Hz, 2H; Por β), 8.76 (d, J = 4.9 Hz, 2H; Por β), 7.71 (d, J = 1.1 Hz, 1H; imidazole H_4), 7.49 (d, J = 1.1 Hz, 1H; imidazole H_5), 6.13 (ddt, J = 17.3, 10.5, 5.7 Hz, 2H; CH_2=C*H*−), 5.46 (ddt, J = 17.3, 3.2, 1.4 Hz, 2H; C*H*$_2$=CH−), 5.30 (ddt, J = 10.5, 3.0, 1.4 Hz, 2H; C*H*$_2$=CH−), 5.06 (br s, 4H; Por-C*H*$_2$), 4.12 (dt, J = 5.7, 1.4 Hz, 4H; CH_2=CHC*H*$_2$−), 3.68 (t, J = 5.7 Hz, 4H; −OC*H*$_2$−), 3.42 (s, 3H; −NCH_3), 2.93–2.71 (m, 4H; Por-

CH_2CH_2-), −2.22 ppm (s, 2H; inner NH); UV/Vis ($CHCl_3$): $\lambda_{max}=444$, 475, 607, 714 nm; fluorescence ($\lambda_{ex}=444$ nm, $CHCl_3$): $\lambda_{em}=721$, 800 nm; MALDI-TOF MS (dithranol): *m/z* calcd for $C_{76}H_{74}N_{12}O_4$: 1219.48 $[M+H^+]$; found: 1219.8.

1,3-Bis(5-(15-(1-methyl-2-imidazolyl)-10,20-bis(3-allyloxypropyl)-zinc-porphyrinyl))butadiyne (3Zn): Compound **6** (15 mg, 12.3 μmol) was dissolved in $CHCl_3$ (10 mL), and a saturated solution (4 mL) of zinc acetate dihydrate in MeOH (27 mg, 123 μmol) was added. After stirring for 2 h, the mixture was washed with brine and water and dried over anhydrous Na_2SO_4. During work-up, precipitates formed. These were washed thoroughly with water and were redissolved in pyridine. The solution was then concentrated by rotary evaporation to give a metallic green-brown filmlike solid (15 mg, 91%). The UV/Vis absorption and fluorescence spectra of polymeric $(\mathbf{3Zn})_n$ were not measured because it was insoluble in $CHCl_3$. However, the UV/Vis absorption and fluorescence spectra of compound **3Zn+2Im** in $CHCl_3$ were measured. The solid $(\mathbf{3Zn})_n$ was dissolved in an excess amount of *N*-methylimidazole. Then a small amount of this solution was dissolved in $CHCl_3$ for measurements. UV/Vis ($CHCl_3$): $\lambda_{max}=455$, 488, 577, 665, 724 nm; fluorescence ($\lambda_{ex}=444$ nm, $CHCl_3$): $\lambda_{em}=734$, 817 nm.

5-Formylisophthalic acid diethyl ester: In a 100-mL flask, which was flushed with N_2, 5-hydroxymethylisophthalic acid diethyl ester (3.6 g, 14.27 mmol) was dissolved in ethanol-free $CHCl_3$ (100 mL) and 4A molecular sieve (eight crystals) was added. Pyridinium chlorochromate (8.4 g, 39 mmol) was added in one portion and the reaction mixture was stirred at RT for 1 h. The mixture was added to vigorously stirred diethyl ether to coagulate the chromium reagent. The solvent was decanted off. The residue was washed two more times with ether. All combined ether layers were passed through Celite until the resulting solution was clear and transparent. TLC of the filtrate showed the presence of the starting material and the crude product was subjected to silica-gel column chromatography to elute the desired compound with *n*-hexane/ethyl acetate (2:1 v/v) to give a pure white solid (2.45 g, 69%). R_f (*n*-hexane/ethyl acetate 2:1) = 0.95; ^{1}H NMR: (270 MHz, $CDCl_3$) $\delta=10.14$ (s, 1H; CHO), 8.92 (t, $J=1.6$ Hz, 1H; Ph-4,6), 8.71 (d, $J=1.6$ Hz, 2H; Ph-2), 4.46 (q, $J=7.3$ Hz, 4H; CH_2), 1.45 ppm (t, $J=7.3$ Hz, 6H; CH_3).

5,15-Bis(3-allyloxypropyl)-10-(3′,5′-diethoxycarbonylphenyl)-20-(1′-methyl-2′-imidazolyl) porphyrin (4): 1-Methyl-1*H*-imidazole-2-carbaldehyde (130 mg, 1.19 mmol), *meso*-(3-allyloxypropyl)dipyrromethane (579 mg, 2.37 mmol), and 5-formylisophthalic acid diethyl ester (297 mg, 1.19 mmol) were dissolved in $CHCl_3$ (500 mL). The mixture was degassed by bubbling with N_2 for 15 min. Then TFA (540 mg, 4.74 mmol) diluted in $CHCl_3$ was added. After stirring for 3.5 h, chloranil (1165 mg, 4.74 mmol) was added. The mixture was then stirred in the dark overnight at RT. The mixture was washed with saturated $NaHCO_3$ solution. The aqueous layer was extracted with $CHCl_3$ and the combined organic layers were washed with brine and water. The resulting crude product was washed with ether and hexane to remove tar and then subjected to silica-gel chromatography to elute compound **4** by using $CHCl_3$/acetone (1:0 to 5:1 v/v). The resulting product was a red-violet solid (101 mg, 11%). However, at this stage, the product still contained some tar that was very difficult to separate, and it was thought appropriate to do purification after zinc insertion. R_f ($CHCl_3$/MeOH 10:1) = 0.54; ^{1}H NMR (270 MHz, $CDCl_3$): $\delta=9.54$ (d, $J=4.9$ Hz, 2H; Por β), 9.50 (d, $J=4.9$ Hz, 2H; Por β), 9.16 (t, $J=1.6$ Hz, 1H; Ph), 9.60 (t, $J=1.6$ Hz, 1H; Ph), 8.96 (t, $J=1.6$ Hz, 1H; Ph), 8.79 (d, $J=4.9$ Hz, 2H; Por β), 8.73 (d, $J=4.9$ Hz, 2H; Por β), 7.69 (d, $J=1.1$ Hz, 1H; imidazole H_4), 7.48 (d, $J=1.1$ Hz, 1H; imidazole H_5), 6.08 (ddt, $J=17.3$, 10.5, 5.7 Hz, 2H; CH_2=C*H*−), 5.41 (ddt, $J=17.3$, 3.2, 1.4 Hz, 2H; CH_2=CH−), 5.26 (ddt, $J=10.5$, 3.0, 1.4 Hz, 2H; CH_2=CH−), 5.10 (t, $J=7.6$ Hz, 4H; Por-CH_2), 4.51 (q, $J=7.3$, 1.4 Hz, 4H; −OCH_2CH$_3$), 4.08 (dt, $J=5.7$, 1.4 Hz, 4H; CH_2=CHCH_2−), 3.66 (t, $J=5.7$ Hz, 4H; −OCH_2−), 3.41 (s, 3H; −NCH$_3$), 2.85–2.72 (m, 4H; Por-CH_2CH_2−), 1.43 (td, $J=7.3$, 1.4 Hz, 6H; −OCH$_2$CH_3), −2.70 ppm (s, 2H; inner NH); MALDI-TOF MS (dithranol): *m/z* calcd for $C_{48}H_{50}N_6O_6$: 806.95 $[M+H^+]$; found: 807.70.

5,15-Bis(3-allyloxypropyl)-10-(3′,5′-diethoxycarbonylphenyl)-20-(1′-methyl-2′-imidazolyl) porphyrinatozinc(II) (4ZnEt): Compound **4** (55 mg, 74.35 μmol) was dissolved in $CHCl_3$ (10 mL) and a saturated solution (4 mL) of zinc acetate dihydrate in MeOH (500 mg/20 mL) was added. After stirring for 1 h, the mixture was washed with sat $NaHCO_3$ solution, brine, and water, and was dried over anhydrous Na_2SO_4. The resulting crude product was purified by chromatography on silica gel with $CHCl_3$/acetone (1:0 to 5:1 v/v) to elute compound **4**, giving a purple solid (46.4 mg, 78%). R_f ($CHCl_3$/acetone 5:1) = 0.85; ^{1}H NMR (270 MHz, $CDCl_3$): $\delta=9.67$ (d, $J=4.6$ Hz, 2H; Por β), 9.57–9.53 (m, 1H; Ph), 9.23–9.20 (m, 1H; Ph), 8.99 (d, $J=4.6$ Hz, 2H; Por β), 8.95–8.92 (m, 1H; Ph), 8.90 (d, $J=4.6$ Hz, 2H; Por β), 6.17 (ddt, $J=17.3$, 10.5, 5.7 Hz, 2H; CH_2=C*H*−), 5.56 (d, $J=1.4$ Hz, 2H; CH_2=CH−), 5.49 (d, $J=1.1$ Hz, 1H; imidazole H_5), 5.44 (d, $J=4.9$ Hz, 2H; Por β), 5.34 (ddt, $J=10.5$, 3.0, 1.4 Hz, 2H; CH_2=CH−), 5.25 (t, $J=5.7$ Hz, 4H; Por-CH_2), 4.69 (q, $J=7.3$, 4H; −OCH_2CH$_3$), 4.48 (q, $J=7.3$, 4H; −OCH_2CH$_3$), 4.24 (dt, $J=5.7$, 1.4 Hz, 4H; CH_2=CHCH_2−), 4.01–3.86 (m, 4H; −OCH_2−), 3.22–2.90 (m, 4H; Por-CH_2CH_2−), 2.14 (d, $J=1.1$ Hz, 1H; imidazole H_4), 1.69 (s, 3H; −NCH$_3$), 1.63 (td, $J=7.3$, 1.4 Hz, 6H; −OCH$_2$CH_3), 1.38 ppm (td, $J=7.3$, 1.4 Hz, 6H; −OCH$_2$CH_3); UV/Vis ($CHCl_3$): $\lambda_{max}=416$, 439, 568, 621 nm; fluorescence ($\lambda_{ex}=439$ nm, $CHCl_3$): $\lambda_{em}=624$, 680 nm; MALDI-TOF MS (dithranol): *m/z* calcd for $C_{48}H_{48}N_6O_6Zn$: 870.32 $[M+H^+]$; found: 870.40.

5,15-Bis(3-allyloxypropyl)-10-[*N*,*N*′-bis-{1,1-(*tert*-butoxycarbonylethyl)-*tert*-butoxycarbonylpropyl}isophthalamido]-20-(1′-methyl-2′-imidazolyl)-porphyrinato zinc(II) (5Zn): Ester compound **4ZnEt** (81 mg, 93.1 μmol) was dissolved in 13:7 THF/MeOH (20 mL) and NaOH aqueous solution (5 mL, 8N). After stirring for 3 h at RT, the solution was acidified with 4N HCl until a pH of 4 was reached, and the solution was extracted with $CHCl_3$. The acidic aqueous layer was neutralized with sat aq $NaHCO_3$ and further extracted with 2:1 $CHCl_3$/THF mixture. All organic layers were dried over anhydrous Na_2SO_4 and concentrated by rotary evaporation to give the carboxylic acid compound **4ZnH** (68 mg, 90%). In a 50 mL flask, compound **4ZnH** (78 mg, 95.7 μmol), benzotriazol-1-yloxytris(dimethylamino)phosphoniumhexafluorophosphate (BOP, 84.6 mg, 191.4 μmol), and diisopropylethylamine (DIPEA, 37.1 mg, 287.1 μmol) were dissolved in dry DMF (8 mL) at RT. After 1 h, tris(*tert*-butoxycarbonylpropyl) amine (100 mg, 239.25 μmol) and DIPEA (24.7 mg, 191.4 μmol) were added and the mixture was stirred for 2 h. After 2 h, the mixture was concentrated, dissolved in $CHCl_3$, washed with brine, and dried over anhydrous Na_2SO_4. The organic layer was concentrated and the crude product was purified by silica-gel column chromatography eluting with $CHCl_3$/acetone (20:1 v/v). After column chromatography, the porphyrin was reprecipitated from a diethyl ether solution by the addition of *n*-hexane to give dendritic porphyrin **5Zn** (138.2 mg, 90%). R_f (Hex/EtOAc 1:1) = 0.75; ^{1}H NMR (600 MHz, $CDCl_3$): $\delta=9.64$ (d, $J=4.2$ Hz, 2H; Por β), 9.33 (s, 1H; Ph), 8.98 (d, $J=4.2$ Hz, 2H; Por β), 8.92 (d, $J=4.2$ Hz, 2H; Por β), 8.73 (s, 1H; Ph), 8.55 (s, 1H; Ph), 7.25 and 7.18 (s, 2H; CONH), 6.19 (ddt, $J=17.4$, 10.8, 5.4 Hz, 2H; CH_2=C*H*−), 5.56 (d, $J=1.8$ Hz, 1H; imidazole H_5), 5.53 (d, $J=17.4$, 3.0, 1.2 Hz, 2H; CH_2=CH−), 5.44 (d, $J=4.2$ Hz, 2H; Por β), 5.34 (ddt, $J=10.8$, 3.0, 1.2 Hz, 2H; CH_2=CH−), 5.28–5.18 (m, 4H; Por-CH_2), 4.24 (dd, $J=5.7$, 1.2 Hz, 4H; CH_2=CHCH_2), 3.99–3.88 (m, 4H; −OCH_2−), 3.16–2.96 (m, 4H; Por-CH_2CH_2−), 2.424 (dt, $J=103.8$, 7.8 Hz, 12H; −NH_2C=(CH_2)$_2$−), 2.189 (dt, $J=93.6$, 7.8 Hz, 13H; −NH_2C=(CH_2)$_2$− and imidazole H_4), 1.69 (s, 3H; −NCH$_3$), 1.53 (s, 27H; *t*Bu), 1.22 ppm (s, 27H; *t*Bu); UV/Vis ($CHCl_3$): $\lambda_{max}=416$, 439, 566, 620 nm; fluorescence ($\lambda_{ex}=439$ nm, $CHCl_3$): $\lambda_{em}=623$, 680 nm; MALDI-TOF MS (dithranol): *m/z* calcd for $C_{88}H_{118}N_8O_{16}Zn$: 1609 $[M+H^+]$; found: 1610.52.

Preparation of tetramer (6_1): Monomer **5Zn** (30 mg, 22.3 μmol) and dimer **3Zn** (72 mg, 44.6 μmol) were dissolved in pyridine (400 mL) for dissociation. After 1 h, pyridine was completely removed and the porphyrins were dissolved in $CHCl_3$ for reorganization, during which, compound $(\mathbf{5Zn})_2$ and oligomeric mixtures $\mathbf{6}_n$ ($n=1$, 2, 3, etc.) were formed. See Supporting Information for the analytical GPC spectrum. The target tetramer $\mathbf{6}_1$ ($n=1$) was roughly separated by preparative GPC (JAI-GEL 3H, eluent: $CHCl_3$; flow rate: 3.5 mL min^{-1}).

Olefin metathesis reaction for covalent linkage of 6_1 (7): Tetramer $\mathbf{6}_1$ (8.9 mg, 1.95 μmol) containing a small amount of dimer $(\mathbf{5Zn})_2$ and hexamer $\mathbf{6}_2$ was dissolved in $CHCl_3$ (2 mL). The Grubbs catalyst (0.72 mg, 0.81 μmol) was added for the metathesis reaction. After 4 h, water was added to terminate the reaction and the target material was extracted

with $CHCl_3$. The combined organic layers were washed with water and brine and dried over anhydrous Na_2SO_4. MALDI-TOF MS (dithranol): *m/z* calcd for $C_{172}H_{228}N_{16}O_{32}Zn_2$: 3162.52 (dimer) $[M+H^+]$; found: 3164.75; *m/z* calcd for $C_{244}H_{290}N_{28}O_{36}Zn_4$: 4452.20 (target tetramer **7**) $[M+H^+]$; found: 4452.64; *m/z* calcd for $C_{316}H_{352}N_{40}O_{40}Zn_6$: 5739.21 (hexamer) $[M+H^+]$; found: 5742.76. Preparative GPC (JAIGEL 3H, eluent: $CHCl_3$; flow rate: 3.5 mL min^{-1}) was performed for further purification/isolation of **7** (7 mg, 80%). Analytical GPC peaks monitored at 300, 350, 420, and 480 nm (JAIGEL 3H-A, eluent: $CHCl_3$; flow rate: 1.2 mL min^{-1}): 12.85 min and (Tosoh TSKgel G2500H_{HR}; eluent: pyridine; flow rate: 1.2 mL min^{-1}): 8.1 min. See Supporting Information for analytical GPC spectra. ^{1}H NMR, split signals due to isomers with respect to two olefin moieties were observed in a ratio of about 1:3. Asterisks (*) and primes (′) indicate signals of major and minor isomers, respectively. No mark indicates that peaks of the isomers (*trans–trans*, *cis–trans*, *cis–cis*) were overlapped. ^{1}H NMR (600 MHz, $CDCl_3$): $\delta = 10.35$–10.28 (*trans* and *cis*, three d, $J = 4.2$ Hz, 4H; Por β), 9.83–9.81 (*trans* and *cis*, three d, $J = 4.2$ Hz, 4H; Por β), 9.59–9.56 (*trans* and *cis*, three d, $J = 4.2$ Hz, 4H; Por β), 9.37* (*trans–trans*, s, 54% × 2H; Ph-4), 9.35′ (*cis–trans*, s, 40% × 2H; Ph-4), 9.33′ (*cis–cis*, s, 6% × 2H; Ph-4), 9.20–8.98 (*trans* and *cis*, six d*, 2 × 4H; Por β), 8.96–8.90 (*trans* and *cis*, three d*, 4H; Por β), 8.74 (br t, $J = 1.8$ Hz, 2H; Ph-2,6), 8.57′ (*cis–cis*, s, 6% × 2H; Ph-2,6), 8.53′ (*cis–trans*, s, 40% × 2H; Ph-2,6), 8.49* (*trans–trans*, s, 54% × 2H; Ph-2,6), 7.19′ (*cis–cis*, s, 6% × 2H; CONH), 7.15′ (*cis–trans*, s, 40% × 2H; CONH), 7.11* (*trans–trans*, s, 54% × 2H; CONH), 6.51* (*trans*, s, 78% × 8H; −CH=), 6.16′ (*cis*, s, 22% × 8H; −CH=), 5.69–5.44 (m, 19H; imidazole-H_5 (4H), Por β (2 × 4H), Por-CH_2′− (44% × 16H)), 5.33–5.11* (br, 56% × 16H; Por-CH_2−), 4.75′ (*cis*, broad, 24% × 16H; −OCH_2CH=), 4.55–4.42* (*trans*, m, 76% × 16H; −OCH_2CH=), 4.4–4.16 (m, 16H; Por-(CH$_2$)$_2$CH_2−), 3.46–2.94 (br m, 16H; Por-CH$_2$CH_2−), 2.59–2.04 (m, 52H; amide ester −CH_2CH_2−(48H), imidazole-H_4 (4H)), 1.83–1.73 (*trans* and *cis*, three d*, $J = 25.2$ Hz, 12H; NCH_3), 1.54 (br s, 54H; *t*Bu), 1.24–1.20 ppm (*trans* and *cis*, three s*, 54H; *t*Bu). Two CONH protons that are unaccounted for overlap with the $CDCl_3$ peak. A * indicates that peaks overlap, which makes the integration ratio difficult to determine. The approximate ratio is 1:6:8. All of these doublet peaks have a coupling constant of $J = 4.2$ Hz; UV/Vis ($CHCl_3$): $\lambda_{max} = 423$, 434, 463, 495, 566, 624, 667, 728 nm; fluorescence ($\lambda_{ex} = 434$ nm, $CHCl_3$): $\lambda_{em} = 738$, 821 nm; MALDI-TOF MS (dithranol): *m/z* calcd for $C_{244}H_{290}N_{28}O_{36}Zn_4$: 4452.20 $[M+H^+]$; found: 4452.69.

Hydrolysis of 7 (7H) and formation of the sodium salt (1): Compound **7** (4.13 mg, 0.93 μmol) was dissolved in formic acid (1 mL). After stirring for 12 h, formic acid was removed by vacuum evaporation. Toluene was added to remove any remaining formic acid azeotropically. The residue was not soluble in any solvent, even water. Therefore, NaOH (12 equiv for the 12 carboxylic acid groups, 0.445 mg, 11.14 μmol) in water (0.1 M) was added to form the sodium salt, which became completely soluble in water. The MALDI-TOF mass spectrum at this stage showed a partial zinc demetalation. Zinc acetate dihydrate (6.12 mg, 27.81 μmol) in water (2 mL) was added. Precipitates formed quickly due to the formation of the zinc carboxylate salt of **7H**. The precipitate was filtered by using a Millipore filter. To obtain the sodium salt, an excess of NaOH (1 mg in 5 mL water) was added. The porphyrin dissolved in water was filtered by using a Millipore filter. HCl (0.1 N) was added very slowly and cautiously to the porphyrin solution until the pH became 5–6 to precipitate compound **7H** in an acid form. The precipitates were collected and washed well with water. Redissolving in alkaline conditions and precipitation in slightly acidic conditions was undertaken twice to remove any water-soluble impurities. Finally, NaOH (12 equiv for the 12 carboxylic acid groups, 0.445 mg, 11.14 μmol) in water (0.1 M) was added and the water was evaporated to afford **1** (3 mg, 85%). UV/Vis (water): $\lambda_{max} = 429$, 490, 571, 619, 670, 735 nm; fluorescence ($\lambda_{ex} = 429$ nm, water): $\lambda_{em} = 748$ nm; MALDI-TOF MS (α-cyano-4-hydroxy cinnamic acid): *m/z* calcd exact mass for $C_{196}H_{194}N_{28}O_{36}Zn_4$: 3779.36 $[M+H^+]$; found: 3780.9.

Two-photon-absorption cross-section measurement:[11b] The effective 2PA cross section $\sigma^{(2)}$ of a 0.4 mM solution of **1** in water was determined by single-beam, open-aperture *Z*-scan measurements with varying incident wavelengths. *Z*-scan measurements were conducted by using an optical parametric oscillator (Continuum Surelight OPO) pumped with a Q-switched Nd:YAG laser (Continuum Surelight I-10), frequency tripled ($\lambda = 355$ nm) from the fundamental wavelength of 1064 nm to give 5-ns pulses (FWHM) with a repetition rate of 10 Hz. The laser intensities were attenuated with a filter to give a peak power of 17 GW cm^{-2}. The laser beam was focused by using a plano-convex lens with a focal length of 100 mm. The samples were placed in a 1-mm quartz cuvette and scanned at a range of 60 mm around the focal point. The data point at each *Z* position was measured with 128 shots.

Singlet-oxygen generation upon two-photon irradiation by ADPA photobleaching:[25,29] Singlet-oxygen generation was monitored by ADPA, a well-known singlet-oxygen scavenger. Stock solutions of 5.0×10^{-5} M ADPA in D_2O, 10^{-4} M TPPS with ADPA in D_2O, and 5.0×10^{-5} M compound **1** with ADPA in D_2O were prepared. The three samples were individually placed in a 1-cm quartz cuvette and illuminated with focused 100-fs pulses (beam waist was around 1 μm) of a mode-locked Ti:sapphire laser (Coherent Mira 900) with a repetition rate of 76 MHz. Two-photon excitation was performed at 890 nm with a peak power of 6.1 GW cm^{-2}.

Acknowledgements

This work was supported by Grant-in-Aid for Scientific Research (A) (No. 15205020) and for Exploratory Research (No. 16655072) from the Ministry of Education, Culture, Sports, Science, and Technology (Monbu Kagakusho), by the Terumo Lifescience Foundation, and by the Iketani Science Technology Foundation. K.O. acknowledges partial financial support from the Kinki-Chiho Invention Center.

[1] a) J. D. Bhawalkar, N. D. Kumar, C. F. Zhao, P. N. Prasad, *J. Clin. Laser Med. Surg.* **1997**, *15*, 201–204; b) E. A. Wachter, W. P. Partridge, W. G. Fisher, H. C. Dees, M. G. Petersen, *Proc. SPIE-Int. Soc. Opt. Eng.* **1998**, *3269*, 68–75; c) J. Liu, Y. W. Zhao, J. Q. Zhao, A. D. Xia, L. J. Jiang, S. Wu, L. Ma, Y. Q. Dong, Y. H. Gu, *J. Photochem. Photobiol. B* **2002**, *68*, 156–164.

[2] a) D. A. Parthenopoulos, P. M. Rentzepis, *Science* **1989**, *245*, 843–845; b) J. H. Strickler, W. W. Webb, *Opt. Lett.* **1991**, *16*, 1780–1782; c) Y. Shen, C. S. Friend, Y. Jiang, D. Jakubczyk, J. Swiatkiewicz, P. N. Prasad, *J. Phys. Chem. B* **2000**, *104*, 7577–7587; d) A. S. Dvornikov, Y. Liang, C. S. Cruse, P. M. Rentzepis, *J. Phys. Chem. B* **2004**, *108*, 8652–8658.

[3] a) D. Day, M. Gu, A. Smallridge, *Opt. Lett.* **1999**, *24*, 948–950; b) H. E. Pudavar, M. P. Joshi, P. N. Prasad, B. A. Reinhardt, *Appl. Phys. Lett.* **1999**, *74*, 1338–1340.

[4] a) C. J. Chang, E. M. Nolan, J. Jaworski, K. Okamoto, Y. Hayashi, M. Sheng, S. J. Lippard, *Inorg. Chem.* **2004**, *43*, 6774–6779; b) S. A. Sanchez, E. Gratton, *Acc. Chem. Res.* **2005**, *38*, 469–477.

[5] a) C. A. Coenjarts, C. K. Ober, *Chem. Mater.* **2004**, *16*, 26, 5556–5558; b) S. Maruo, O. Nakamura, S. Kawata, *Opt. Lett.* **1997**, *22*, 132–134; c) W. Zhou, S. M. Kuebler, K. L. Braun, T. Yu, J. K. Cammack, C. K. Ober, J. W. Perry, S. R. Marder, *Science* **2002**, *296*, 1106–1109.

[6] M. Göppert-Mayer, *Annalen der Physik* **1931**, *9*, 273–295.

[7] a) D. E. J. G. J. Dolmans, D. Fukumura, R. K. Jain, *Nat. Rev. Cancer* **2003**, *3*, 380–387; b) A. Karotki, M. Drobizhev, M. Kruk, C. Spangler, E. Nickel, N. Mamardashvili, A. Rebane, *J. Opt. Soc. Am. B* **2003**, *20*, 321–332.

[8] a) J. D. Bhawalkar, G. S. He, P. N. Prasad, *Rep. Prog. Phys.* **1996**, *59*, 1041–1070; b) M. Drobizhev, A. Rebane, A. Karotki, C. W. Spangler, *Recent Res. Dev. Appl. Phys.* **2001**, *4*, 1–26.

[9] a) M. Albota, D. Beljonne, J. Bredas, J. Ehrlich, J. Fu, A. Heikal, S. Hess, T. Kogej, M. Levin, S. Marder, D. McCord-Maughon, J. Perry, H. Rockel, M. Rumi, G. Subramaniam, W. Webb, X. Wu, C. Xu, *Science* **1998**, *281*, 1653–1656; b) B. Reinhardt, L. Brott, S. Clarson, A. Dillard, J. Bhatt, R. Kannan, L. Yuan, G. He, P. N. Prasad, *Chem. Mater.* **1998**, *10*, 1863–1874; c) C. Wang, P. Macak, Y. Luo, H. Agren, *J. Chem. Phys.* **2001**, *114*, 22, 9813–9820; d) K. Kamada, K.

Ohta, Y. Iwase, K. Kondo, *Chem. Phys. Lett.* **2003**, *372*, 386–393; e) J. Tanihara, K. Ogawa, Y. Kobuke, *J. Photochem. Photobiol. A* **2006**, *178*, 140–149.

[10] a) M. Drobizhev, A. Karotki, M. Kruk, A. Rebane, *Chem. Phys. Lett.* **2002**, *355*, 175–182; b) M. Drobizhev, A. Karotki, M. Kruk, N. Z. Mamardashvili, A. Rebane, *Chem. Phys. Lett.* **2002**, *361*, 504–512; c) M. Drobizhev, A. Karotki, M. Kruk, A. Krivokapic, H. L. Anderson, A. Rebane, *Chem. Phys. Lett.* **2003**, *380*, 690–699.

[11] a) K. Ogawa, A. Ohashi, Y. Kobuke, K. Kamada, K. Ohta, *J. Am. Chem. Soc.* **2003**, *125*, 13356–13357; b) K. Ogawa, A. Ohashi, Y. Kobuke, K. Kamada, K. Ohta, *J. Phys. Chem. B* **2005**, *109*, 22003–22012.

[12] Y. Kobuke, H. Miyaji, *J. Am. Chem. Soc.* **1994**, *116*, 4111–4112.

[13] a) A. Karotki, M. Drobizhev, Y. Dzenis, P. N. Taylor, H. L. Anderson, A. Rebane, *Phys. Chem. Chem. Phys.* **2004**, *6*, 7–10; b) M. Drobizhev, Y. Stepanenko, Y. Dzenis, A. Karotki, A. Rebane, P. N. Taylor, H. L. Anderson, *J. Am. Chem. Soc.* **2004**, *126*, 15352–15353.

[14] a) J. Moan, Q. Peng in *Photodynamic Therapy* (Ed.: T. Patrice), The Royal Society of Chemistry, Cambridge, **2004**, pp. 3–13; b) J. Moan, *Photochem. Photobiol.* **1986**, *43*, 6, 681–690; c) J. Moan, K. Berg, *Photochem. Photobiol.* **1992**, *55*, 6, 931–948; d) Y. N. Konan, R. Gurny, E. Allemann, *J. Photochem. Photobiol. B* **2002**, *66*, 89–106; e) P. Nyman, P. H. Hynninen, *J. Photochem. Photobiol B* **2004**, *73*, 1–28; f) K. Ogawa, H. Hasegawa, Y. Inaba, Y. Kobuke, H. Inouye, Y. Kanemitsu, E. Kohno, T. Hirano, S.-I. Ogura, I. Okura, *J. Med. Chem.* **2006**, *49*, 2276–2283.

[15] I. J. Macdonald, T. J. Dougherty, *J. Porphyrins Phthalocyanines* **2001**, *5*, 105–129.

[16] A. J. Welch, M. J. C. van Gemert in *Electro-Optics Handbook* (Eds.: R. W. Waynant, M. N. Ediger), McGraw-Hill, New York, **1993**, pp. 24.1–24.29.

[17] a) P. K. Frederiksen, S. P. McIlroy, C. B. Nielsen, L. Nikolajsen, E. Skovsen, M. Jorgensen, K. V. Mikkelsen, P. R. Ogilby, *J. Am. Chem. Soc.* **2005**, *127*, 255–269; b) T. D. Poulsen, P. K. Frederiksen, M. Jorgensen, K. V. Mikkelsen, P. R. Ogilby, *J. Phys. Chem. A* **2001**, *105*, 11488–11495; c) J. Arnbjerg, M. Johnsen, P. K. Frederiksen, S. E. Braslavsky, P. R. Ogilby, *J. Phys. Chem. A* **2006**, *110*, 7375–7385; d) S. P. McIlroy, E. Clo, L. Nikolajsen, P. K. Frederiksen, C. B. Nielsen, K. V. Mikkelsen, K. V. Gothelf, P. R. Ogilby, *J. Org. Chem.* **2005**, *70*, 1134–1146.

[18] a) K. König, *J. Microsc.* **2000**, *263*, 88–97; b) B. A. King, D. H. Oh, *Photochem. Photobiol.* **2004**, *80*, 1–6, and references therein.

[19] a) G. R. Newkome, R. K. Behera, C. N. Moorefield, G. R. Baker, *J. Org. Chem.* **1991**, *56*, 7162–7167; b) A. Ohashi, A. Satake, Y. Kobuke, *Bull. Chem. Soc. Jpn.* **2004**, *77*, 365–374.

[20] a) K. Ogawa, Y. Kobuke, *Angew. Chem.* **2000**, *112*, 4236–4239; *Angew. Chem. Int. Ed.* **2000**, *39*, 4070–4073; b) Y. Kobuke, K. Ogawa, *Bull. Chem. Soc. Jpn.* **2003**, *76*, 4, 689–708.

[21] a) J. J. Piet, P. N. Taylor, B. R. Wegewijs, H. L. Anderson, A. Osuka, J. M. Warman, *J. Phys. Chem. B* **2001**, *105*, 97–104; b) H. L. Anderson, *Inorg. Chem.* **1994**, *33*, 972–981; c) V. S. -Y. Lin, S. G. DiMagno, M. J. Therien, *Science* **1994**, *264*, 1105–1111; d) S. M. LeCours, H. W. Guan, S. G. DiMagno, C. H. Wang, M. J. Therien, *J. Am. Chem. Soc.* **1996**, *118*, 1492–1503; e) S. Priyadarshy, M. J. Therien, D. N. Beratan, *J. Am. Chem. Soc.* **1996**, *118*, 1504–1510.

[22] a) W. R. Dichtel, J. M. Serin, C. Edder, J. M. J. Frechet, M. Matuszewki, L. Tan, T. Y. Ohulchanskyy, P. N. Prasad, *J. Am. Chem. Soc.* **2004**, *126*, 17, 5380–5381; b) D. N. Brousmiche, J. M. Serin, J. M. J. Frechet, G. S. He, T. C. Lin, S. J. Chung, P. N. Prasad, *J. Am. Chem. Soc.* **2003**, *125*, 1445–1449.

[23] A. Miura, Y. Shibata, H. Chosrowjan, N. Mataga, N. Tamai, *J. Photochem. Photobiol. A* **2006**, *178*, 192–200, and references therein.

[24] K. Ogawa, J. Dy, Y. Kobuke, *J. Porphyrins Phthalocyanines* **2005**, *9*, 735–744.

[25] M. A. Oar, J. M. Serin, W. R. Dichtel, J. M. J. Frechet, T. Y. Ohulchanskyy, P. N. Prasad, *Chem. Mater.* **2005**, *17*, 2267–2275.

[26] a) P. R. Ogilby, C. S. Foote, *J. Am. Chem. Soc.* **1981**, *103*, 1219–1221; b) T. A. Jenny, N. J. Turro, *Tetrahedron Lett.* **1982**, *23*, 2923–2926; c) F. Wilkinson, W. P. Helman, A. B. Ross, *J. Phys. Chem. Ref. Data* **1995**, *24*, 663–677.

[27] a) R. Schmidt, *J. Am. Chem. Soc.* **1989**, *111*, 6983–6987; b) M. A. J. Rodgers, *J. Am. Chem. Soc.* **1983**, *105*, 6201–6205; c) R. Schmidt, E. Afshari, *Ber. Bunsenges. Phys. Chem.* **1992**, *96*, 788–794; d) J. Davila, A. Harriman, *Photochem. Photobiol.* **1990**, *51*, 9–19.

[28] a) L. R. Milgrom, P. J. F. Dempsey, G. Yahioglu, *Tetrahedron* **1996**, *52*, 9877–9890; b) C. Ikeda, A. Satake, Y. Kobuke, *Org. Lett.* **2003**, *5*, 4935–4938; c) F. Hajjaj, Z. S. Yoon, M.-C. Yoon, J. Park, A. Satake, D. Kim, Y. Kobuke, *J. Am. Chem. Soc.* **2006**, *128*, 4612–4623; d) W. Fudickar, J. Zimmermann, L. Ruhlmann, J. Schneider, B. Roder, U. Siggel, J. H. Fuhrhop, *J. Am. Chem. Soc.* **1999**, *121*, 9539–9545.

[29] B. A. Lindig, M. A. J. Rodgers, P. Schaap, *J. Am. Chem. Soc.* **1980**, *102*, 5590–5593.

Received: August 19, 2006
Published online: January 16, 2007

